Chemistry of Iron with Dipicolinic Acid. 3. Heptacoordinated Iron in $[(dipicH)_2Fe^{II}(OH_2)]$ and $[(dipic)_2Fe^{II}_2(OH_2)_6]\cdot 2dipicH_2$

P. Lainé,[†] A. Gourdon,*[,†] J.-P. Launay,[†] and J.-P. Tuchagues[‡]

Molecular Electronics Group, CEMES, CNRS UP8011, BP4347, 29 Rue J. Marvig, 31055 Toulouse Cedex, France, and Laboratoire de Chimie de Coordination du CNRS, UP8241 liée par conventions à l'Université Paul Sabatier et à l'Institut National Polytechnique, 205 route de Narbonne, 31077 Toulouse Cedex, France

Received January 27, 1995[⊗]

Reaction of 2,6-pyridinedicarboxylic acid (dipicolinic acid, $dipicH_2$) with Mohr's salt at pH 5.65 afforded $[(dipic)_{10}(dipicH)_6Fe^{II}_{13}(OH_2)_{24}]\cdot 13H_2O$, which slowly decomposed to a heptacoordinated mononuclear complex (**1**): $[(dipicH)_2Fe^{II}(OH_2)]$. Acidification of $[(dipic)_2Fe^{II}]Na_2\cdot 2H_2O$ yielded $[(dipic)_2(dipicH_2)_2Fe^{II}_3(OH_2)_4]$, which decomposed to afford the heptacoordinated dinuclear complex $[(dipic)_2Fe^{II}_2(OH_2)_6]\cdot 2dipicH_2$ (**2**). $\mathbf{1}\cdot 3H_2O$ crystallized in the monoclinic space group $P2_1/n$ with $a = 6.996(2)$ Å, $b = 23.898(6)$ Å, $c = 10.728(3)$ Å, $\beta = 100.25(5)°$, $V = 1765(4)$ Å^3 and $Z = 4$. **2** crystallized in the monoclinic space group $P2_1/c$ with $a = 9.095(6)$ Å, $b = 14.50(1)$ Å, $c = 12.16(3)$ Å, $\beta = 97.28(4)°$, $V = 1591(4)$ Å^3, and $Z = 2$. Analysis of the thermal variation of the magnetic susceptibility of **2** indicates the presence of weak antiferromagnetic interactions ($J = -3.4$ cm^{-1}, $H = -2JS_1S_2$) of the same order of magnitude as the single-ion zero-field splitting of heptacoordinated iron(II) (-3.1 cm^{-1}) in this dinuclear complex.

Introduction

Heptacoordination is a well-known coordination mode. However examples with iron(II) are rather rare. It has been observed with pentadentate ligands maintaining five coordination sites in one plane and allowing two axial coordinations; so far, all the structurally characterized Fe^{II} heptacoordinated complexes[1] were 2,6-diacetylpyridine diimine macrocyclic derivatives[2] or crown ether derivatives.[3] In the case of $dipicH_2$ (2,6-pyridine dicarboxylic acid, dipicolinic acid) or substituted $dipicH_2$ complexes, some cases of heptacoordination are reported in μ-hydroxo dimers of iron(III)[4] and of chromium(III)[5] in peroxo complexes of titanium,[6] or hydroxylamino-*N*,*O* complexes of vanadium.[7]

During the course of our studies of the dipicolinic acid/iron(II) system,[8] we have explored the compounds obtained by acidic *degradation* of $[(dipic)_2Fe^{II}]^{2-}$ or deriving formally from this species. We thus obtained two new complexes $[(dipicH)_2Fe^{II}(OH_2)]$ (**1**) and $[(dipic)_2Fe^{II}_2(OH_2)_6]\cdot 2dipicH_2$ (**2**), which were shown to be heptacoordinated by X-ray crystallography. Their structures and magnetic properties are discussed, and the magnetic properties of the dinuclear complex **2** are studied.

Experimental Section

Most experimental details have been described in previous papers of this issue.[8]

Variable-temperature magnetic susceptibility data were obtained on powdered polycrystalline samples with a Quantum Design MPMS SQUID susceptometer. Diamagnetic corrections were applied by using Pascal's constants. Least-squares computer fittings of the magnetic susceptibility data were accomplished with an adapted version of the function-minimization program STEPT.[9]

Synthesis of $[(dipicH)_2Fe^{II}(OH_2)]$. A suspension of $dipicH_2$ (9.75 g, 58.34 mmol) in degassed water (75 mL) at room temperature was treated with concentrated aqueous NaOH up to pH = 5.65 (final volume *ca.* 100 mL). A 17.25 g sample of Mohr's salt (43.99 mmol) was added to the refluxing solution. After 10 min of stirring at this temperature, the dark-red mixture was left to cool to room temperature. At this temperature, the pH was then found to be 1.95. After 12 h at room temperature, filtration gave 9.60 g of red-violet crystals of $[(dipic)_{10}(dipicH)_6Fe^{II}_{13}(OH_2)_{24}]\cdot 13H_2O$. Cooling of the mother liquor to 4 °C provided 1.6 g of orange crystals of $[(dipicH)_2Fe^{II}(OH_2)]\cdot 3H_2O$ (yield 4.4%). Anal. Calcd for $C_{14}H_{16}N_2FeO_{12}$: C, 36.54; H, 3.50; N, 6.09; Fe, 12.13. Found: C, 36.29; H, 3.34; N, 6.10; Fe, 11.68. FTIR (KBr pellets, cm^{-1}): 3389 (ν OH); 1723 (ν_{asym} COO from COOH); 1659, 1625, 1588 (ν_{asym} COO); 1462, 1379, 1333 (ν_{sym} COO$^-$). When the crystals of $[(dipic)_{10}(dipicH)_6Fe^{II}_{13}(OH_2)_{24}]\cdot 13H_2O$ are not collected in due time and left in the mother liquor, a much higher yield (*ca.* 55%) of less pure product can obtained.

Synthesis of $[(dipic)_2Fe^{II}_2(OH_2)_6]\cdot 2dipicH_2$. $[(dipic)_2Fe^{II}]Na_2\cdot 2H_2O$ (1 g, 2.14 mmol) was dissolved under argon in degassed boiling water

[†] CEMES.

[‡] Laboratoire de Chimie de Coordination du CNRS.

[⊗] Abstract published in *Advance ACS Abstracts,* September 1, 1995.

(1) Cambridge Structural Database, release Oct 1994. Allen, F. H.; Kennard, O.; Taylor, R. *Acc. Chem. Res.* **1983**, *16*, 146.

(2) (a) Drew, M. G. B.; Bin Othman, A. H.; McIlroy, P.; Nelson, S. M. *Acta Crystallogr., B* **1976**, *32*, 1029. (b) Dessy, G.; Fares, V. *Cryst. Struct. Commun.* **1981**, *10*, 1025. Palenik, G. J.; Wester, D. W. *Inorg. Chem.* **1978**, *17*, 864. (c) Bishop, M. M.; Lewis, J.; O'Donoghue, T. D.; Raithby, P. R.; Ramdsen, J. N. *J. Chem. Soc., Chem. Commun.* **1978**, 828. (d) Bishop, M. M.; Lewis, J.; O'Donoghue, T. D.; Raithby, P. R.; Ramdsen, J. N. *J. Chem. Soc., Dalton Trans.* **1980**, 1390. (e) Drew, M. G. B.; Bin Othman, A. H.; Nelson, S. M. *J. Chem. Soc., Dalton Trans.* **1976**, 1394. (f) Bonardi, A.; Carini, C.; Merlo, C.; Pelizzi, G.; Tarasconi, P.; Vitali, F.; Cavatorta, F. *J. Chem. Soc., Dalton Trans.* **1990**, 2771.

(3) Larson, S. B.; Simonsen, S. H.; Ramdsen, J. N.; Lagowski, J. J. *Acta Crystallogr., C* **1990**, *46*, 1930.

(4) (a) Ou, C. C.; Lalancette, R. A.; Potenza, J. A.; Schugar, H. J. *J. Am. Chem. Soc.* **1978**, *100*, 2053. (b) Tich, J. A.; Ou, C. C.; Powers, D.; Vasiliou, B.; Mastropaolo, D.; Potenza, J. A.; Schugar, H. J. *J. Am. Chem. Soc.* **1976**, *98*, 1425.

(5) Cline, S. J.; Kallesoe, S.; Pedersen, E.; Hodgson, D. J. *Inorg. Chem.* **1979**, *18*, 796.

(6) (a) Schwarzenbach, D. *Helv. Chim. Acta* **1972**, *55*, 2990. (b) Schwarzenbach, D. *Inorg. Chem.* **1970**, *9*, 2391. (c) Manohar, H.; Schwarzenbach, D. *Helv. Chim. Acta* **1974**, *57*, 1086.

(7) Wieghardt, K.; Quilitzsch, U.; Nuber, B.; Weiss, J. *Angew. Chem., Int. Ed. Engl.* **1978**, *17*, 351.

(8) Lainé, P.; Gourdon, A.; Launay, J.-P. *Inorg. Chem.* **1995**, *34*, 5129, 5138.

(9) Chandler, J. P. Quantum Chemistry Program Exchange, Indiana University, 1973; Program 66.

0020-1669/95/1334-5150$09.00/0

Table 1. Crystal Data for $[(dipicH)_2Fe^{II}(OH_2)]\cdot 3H_2O$ (**1**) and $[(dipic)_2Fe^{II}_2(OH_2)_6]\cdot 2dipicH_2$ (**2**)

	1	**2**
formula	$C_{14}H_{16}N_2FeO_{12}$	$C_{28}H_{28}N_4Fe_2O_{22}$
fw	460.13	884.24
space group	$P2_1/n$ (No. 14)	$P2_1/c$ (No. 14)
a, Å	6.996(2)	9.095(6)
b, Å	23.898(6)	14.50(1)
c, Å	10.728(3)	12.16(3)
β, deg	100.25(5)	97.28(4)
V, Å^3	1765(4)	1591(4)
Z	4	2
T, °C	21	21
μ(Mo K$_\alpha$), cm^{-1}	9.21	10.13
ϱ_{calcd}, g cm^{-3}	1.73	1.85
R^a	0.0369	0.0348
$R_w{}^b$	0.0435	0.0378

$^a R = \Sigma||F_o| - |F_c||/\Sigma|F_o|$. $^b R_w = [\Sigma w(|F_o| - |F_c|)^2/\Sigma w|F_o|^2]^{1/2}$.

Table 2. Selected Atomic Coordinates and Equivalent Isotropic Thermal Parameters (Å^2) for $[(dipicH)_2Fe^{II}(OH_2)]\cdot 3H_2O$ (**1**)

atom	*x/a*	*y/b*	*z/c*	*U*(iso)^a
Fe(1)	0.14169(6)	0.87933(2)	0.82899(4)	0.0280
N(1)	0.1034(3)	0.79140(9)	0.8117(2)	0.0258
C(1)	0.4254(4)	0.7796(1)	0.9216(3)	0.0317
C(2)	0.2359(4)	0.7541(1)	0.8589(3)	0.0288
C(3)	0.1997(4)	0.6973(1)	0.8529(3)	0.0370
C(4)	0.0166(5)	0.6798(1)	0.7977(4)	0.0384
C(5)	−0.1243(4)	0.7186(1)	0.7511(3)	0.0356
C(6)	−0.0745(4)	0.7746(1)	0.7585(2)	0.0270
C(7)	−0.2122(4)	0.8216(1)	0.7110(2)	0.0268
O(11)	0.4453(3)	0.83004(8)	0.9291(2)	0.0361
O(12)	0.5542(3)	0.7425(1)	0.9650(3)	0.0425
O(71)	−0.1409(3)	0.87069(7)	0.7221(2)	0.0313
O(72)	−0.3828(3)	0.81077(8)	0.6657(2)	0.0368
N(11)	0.1945(3)	0.95981(9)	0.9249(2)	0.0249
C(11)	0.1324(4)	0.9020(1)	1.0972(3)	0.0270
C(12)	0.2032(4)	0.9564(1)	1.0499(3)	0.0259
C(13)	0.2645(4)	1.0004(1)	1.1314(3)	0.0322
C(14)	0.3192(4)	1.0498(1)	1.0812(3)	0.0332
C(15)	0.3055(4)	1.0544(1)	0.9519(3)	0.0306
C(16)	0.2410(4)	1.0088(1)	0.8764(3)	0.0278
C(17)	0.2042(4)	1.0116(1)	0.7357(3)	0.0317
O(111)	0.0792(3)	0.86577(8)	1.0111(2)	0.0325
O(112)	0.1245(3)	0.89648(9)	1.2094(2)	0.0396
O(171)	0.0969(3)	0.98014(9)	0.6708(2)	0.0424
O(172)	0.2986(4)	1.0527(1)	0.6937(2)	0.0477
O(110)	0.3108	0.8821	0.6881	0.0443

^{a} Equivalent isotropic *U*(iso) defined as one-third of the trace of the orthogonalized tensor.

(40 mL). The solution was then concentrated to 15 mL by distillation and treated by dropwise addition of 0.1 M degassed aqueous HCl. The addition was stopped when the initially deep red solution cleared. The resulting solution was then left to cool. Dark red needles of $[(dipic)_2(dipicH)_2Fe^{II}_3(OH_2)_4]$,[8] which were initially formed, turned into deep red-orange crystals of $[(dipic)_2Fe^{II}_2(OH_2)_6]\cdot 2dipicH_2$. After 36 h at room temperature, the pH was 1.35 and the product was filtered off. The crystals of **2** were subsequently manually picked over the white $dipicH_2$ crystals (90 mg, 9.5%). Anal. Calcd for $C_{28}H_{28}N_4Fe_2O_{22}$: C, 38.03; H, 3.19; N, 6.33; Fe, 12.63. Found: C, 37.99; H, 3.20; N, 6.31; Fe, 12.61. FTIR (KBr pellets, cm^{-1}): 3411, 3250, 3105 (ν OH); 1692 (ν_{asym} COO from COOH); 1660, 1621, 1593 (ν_{asym} COO from COO$^-$); 1463, 1424, 1400 (ν_{sym} COO$^-$).

X-ray Crystallography. Single-crystal X-ray diffraction experimental details have been described in a previous paper.[8] Crystal data for $[(dipicH)_2Fe^{II}(OH_2)]$ and $[(dipic)_2Fe^{II}_2(OH_2)_6]\cdot 2dipicH_2$ are summarized in Table 1. Selected atomic coordinates are given in Tables 2 and 5. Selected bond lengths and angles are given in Tables 3 and 6, respectively.

Table 3. Selected Bond Distances (Å) and Angles (deg) for $[(dipicH)_2Fe^{II}(OH_2)]\cdot 3H_2O$ (**1**)

Fe(1)−N(1)	2.122(2)	C(1)−O(12)	1.292(3)
Fe(1)−O(11)	2.498(2)	C(7)−O(71)	1.273(3)
Fe(1)−O(71)	2.112(2)	C(7)−O(72)	1.233(3)
Fe(1)−N(11)	2.182(2)	C(11)−O(111)	1.273(3)
Fe(1)−O(111)	2.102(2)	C(11)−O(112)	1.222(3)
Fe(1)−O(171)	2.932(2)	C(17)−O(171)	1.194(4)
Fe(1)−O(110)	2.0793(4)	C(17)−O(172)	1.309(4)
C(1)−O(11)	1.213(3)		

O(11)−Fe(1)−N(1)	69.83(7)	O(171)−Fe(1)−O(11)	129.16(6)
O(71)−Fe(1)−N(1)	76.37(7)	O(171)−Fe(1)−O(71)	76.85(7)
O(71)−Fe(1)−O(11)	146.06(7)	O(171)−Fe(1)−N(11)	62.62(7)
N(11)−Fe(1)−N(1)	157.28(8)	O(110)−Fe(1)−N(1)	92.71(6)
N(11)−Fe(1)−O(11)	98.81(7)	O(110)−Fe(1)−O(11)	77.14(5)
N(11)−Fe(1)−O(71)	113.95(7)	O(110)−Fe(1)−O(71)	101.95(6)
O(111)−Fe(1)−N(1)	83.38(8)	O(110)−Fe(1)−N(11)	104.12(6)
O(111)−Fe(1)−O(11)	80.17(8)	O(171)−Fe(1)−O(111)	130.27(7)
O(111)−Fe(1)−O(71)	99.23(8)	O(110)−Fe(1)−O(111)	156.91(6)
O(111)−Fe(1)−N(11)	75.13(8)	O(110)−Fe(1)−O(171)	64.47(5)
O(171)−Fe(1)−N(1)	139.84(7)		

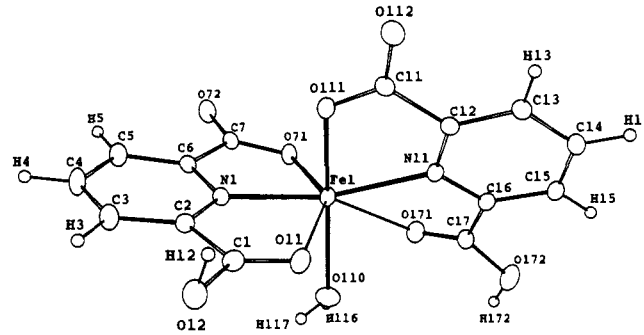

Figure 1. ORTEP drawing of $[(dipicH)_2Fe^{II}(OH_2)]$ (**1**).

Results and Discussion

$[(dipicH)_2Fe^{II}(OH_2)]$ (1). While studying the reactions between $dipicH_2$ and Fe^{II} at various pHs,[8] we obtained a crystalline solid of overall formula $[(dipic)_{10}(dipicH)_6Fe^{II}_{13}(OH_2)_{24}]\cdot 13H_2O$ containing in the same unit cell one trinuclear complex, two types of dinuclear complexes, and two mononuclear complexes. This synthesis was performed with a solution of "$dipicH_2$" in hot water at pH = 5.65 (in fact mainly $dipicH^-$). Addition of Mohr's salt and cooling (the pH was then 1.95) gave a first crop of purplish-blue crystals of this Fe^{II}_{13} compound (70% yield). Further cooling gave after 48 h orange crystals of $[(dipicH)_2Fe^{II}(OH_2)]$. It must be emphasized that, very surprisingly, *if the first crop is not collected in due time, the dark-purplish crystals of* $[(dipic)_{10}(dipicH)_6Fe^{II}_{13}(OH_2)_{24}]\cdot 13H_2O$ *turn into orange crystals of the* $[(dipicH)_2Fe^{II}(OH_2)]$ *type.* This is not a trivial process, because crystals of the first type *dissolve* while crystals of the second type appear.

Although the exact reasons for this strange behavior are not fully understood, we shall notice that the reaction of Fe^{2+} with $dipicH^-$ releases protons. This is why the pH of the solution becomes very acidic (1.95). During the crystallization of $[(dipic)_{10}(dipicH)_6Fe^{II}_{13}(OH_2)_{24}]\cdot 13H_2O$, the pH decreases sufficiently to finally pull this species out of equilibrium. $[(dipic)_{10}(dipicH)_6Fe^{II}_{13}(OH_2)_{24}]\cdot 13H_2O$ is thus converted into the more acidic form $[(dipicH)_2Fe^{II}(OH_2)]$ ("more acidic" meaning that, in this second species, all the dipic ligands are protonated). Thus it seems that crystals of the first crop are favored kinetically while crystals of the second are favored thermodynamically. Once crystals of the first crop are formed, their conversion into the more stable crystals of the second crop cannot be fast because it needs redissolution and recrystallization steps.

Figure 1 depicts the structure of the complex. The iron atom is surrounded by two $dipicH^-$ ligands and one water molecule.

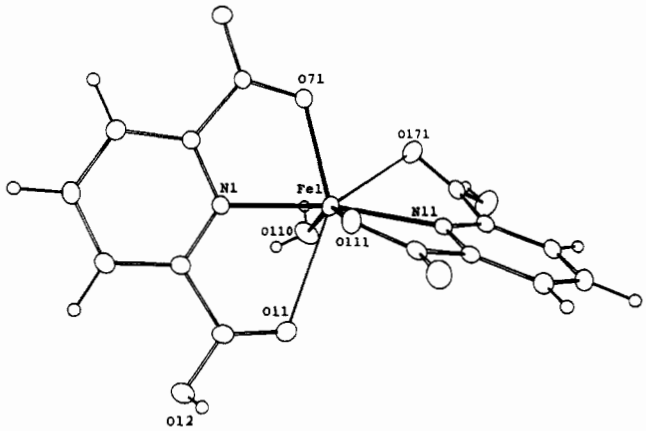

Figure 2. View of the iron coordination geometry in **1** showing the nonplanarity of one of the dipic ligands.

Table 4. Hydrogen Bond Distances in $[(dipicH)_2Fe^{II}(OH_2)]$ (Å)

O(71)−H(301)	2.00(5)	O(71)−O(300)	2.780(3)
O(72)−H(101)	2.04(5)	O(72)−O(100)	2.747(3)
O(72)−H(117)	2.07(5)	O(72)−O(110)	2.782(2)
O(112)−H(201)	1.82(5)	O(112)−O(200)	2.761(3)
O(200)−H(116)	1.99(5)	O(200)−O(110)	2.716(3)
O(300)−H(172)	1.68(5)	O(300)−O(172)	2.563(4)

The geometry can be described as a distorted octahedron (see Figure 2) with introduction of O(171) in the triangular face defined by O(71), N(11), and O(110). Five Fe−O and Fe−N bond lengths are similar to those observed in other $[(dipic)_2Fe^{II}]$ complexes.[8] The two longer Fe−O distances correspond to the protonated carboxylates of O(11) and O(171) with Fe(1)−O(11) = 2.498(2) Å and Fe(1)−O(171) = 2.932(2) Å. The O(171) and O(172) atoms lie 0.45 and 0.26 Å from the dipic mean plane, respectively.

As shown by the distances given in Table 4, the crystal packing results from six intermolecular hydrogen bonds between adjacent molecules related by symmetry operators.

In order to compare this dark-red complex $[(dipicH)_2Fe^{II}(OH_2)]$ with the green compound described in ref 10 as $[(dipicH)_2Fe^{II}]\cdot 2H_2O$, we have undertaken the synthesis of this latter compound according to the published experimental procedure. However, and according to UV−vis and FTIR spectra, chemical analyses, and X-ray data, this green compound should be formulated as the Fe^{III} unprotonated complex $[(dipic)_2Fe^{III}](H_5O_2)$,[11] and *not* as a doubly protonated Fe^{II} complex.

$[(dipic)_2Fe^{II}_2(OH_2)_6]\cdot 2dipicH_2$ (2). In a reaction similar to that described for **1**, acidification of a saturated hot aqueous solution of $[(dipic)_2Fe^{II}]Na_2\cdot 2H_2O$ by diluted hydrochloric acid rapidly afforded dark red needles of $[(dipic)_2(dipicH)_2Fe^{II}_3(OH_2)_4]$,[8] which slowly became a mixture of orange crystals of $[(dipic)_2Fe^{II}_2(OH_2)_6]\cdot 2dipicH_2$ and white crystals of $dipicH_2$. Thus, as in the previous reaction leading to **1**, the formation of a first type of crystals and their subsequent conversion to a second type are observed.

The compound crystallizes in the centrosymetric space group $P2_1/c$. The asymmetric unit contains half a molecule of $[(dipic)Fe^{II}(OH_2)_3]_2$ centered on the origin (Figure 3) and one molecule of $dipicH_2$ in general position. The centrosymmetric complex is composed of two $[(dipic)Fe^{II}(OH_2)_3]$ fragments asymmetrically bridged by oxygen atoms belonging to two carboxylate groups with distances O(11)−Fe(1) = 2.208(2) Å and O(11)−Fe(1)′ = 2.307(2) Å (Table 6). In each fragment, the iron atom is heptacoordinated in a pentagonal bipyramidal geometry. The atoms of the dipic ligand O(11), N(1), O(71), the iron atom,

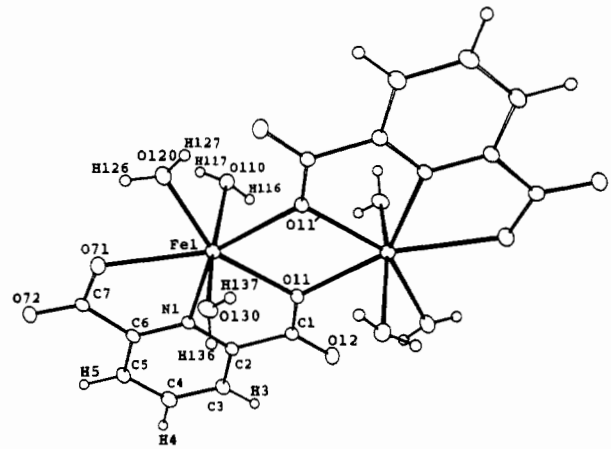

Figure 3. Molecular drawing of the complex $[(dipic)_2Fe^{II}_2(OH_2)_6]$.

Table 5. Selected Positional and Equivalent Isotropic Thermal Parameters (Å²) for $[(dipic)_2Fe^{II}_2(OH_2)_6]\cdot 2dipicH_2$ (**2**)

atom	*x/a*	*y/b*	*z/c*	*U*(iso)[a]
Fe(1)	0.42200(6)	0.41454(4)	0.09112(5)	0.0245
N(1)	0.5148(3)	0.2775(2)	0.0574(2)	0.0206
C(1)	0.6273(4)	0.3629(3)	−0.0773(3)	0.0216
C(2)	0.5977(4)	0.2725(3)	−0.0247(3)	0.0211
C(3)	0.6583(5)	0.1910(3)	−0.0573(3)	0.0285
C(4)	0.6316(5)	0.1116(3)	−0.0019(4)	0.0319
C(5)	0.5469(5)	0.1154(3)	0.0842(3)	0.0288
C(6)	0.4883(4)	0.1996(2)	0.1104(3)	0.0216
C(7)	0.3946(4)	0.2095(3)	0.2024(3)	0.0220
O(11)	0.5704(3)	0.4331(2)	−0.0374(2)	0.0223
O(12)	0.7027(3)	0.3621(2)	−0.1551(2)	0.0301
O(71)	0.3503(3)	0.2915(2)	0.2165(2)	0.0316
O(72)	0.3637(3)	0.1418(2)	0.2559(2)	0.0301
O(110)	0.2288(3)	0.4042(2)	−0.0470(2)	0.0297
O(120)	0.2572(4)	0.4630(2)	0.1824(3)	0.0333
O(130)	0.5863(3)	0.4564(2)	0.2222(3)	0.0317
N(11)	0.0452(3)	0.2414(2)	0.5362(3)	0.0243
C(11)	0.1680(4)	0.3489(3)	0.4257(3)	0.0262
C(12)	0.0869(4)	0.3295(3)	0.5225(3)	0.0246
C(13)	0.0566(5)	0.3997(3)	0.5922(3)	0.0311
C(14)	−0.0165(5)	0.3807(3)	0.6809(4)	0.0366
C(15)	−0.0601(5)	0.2911(3)	0.6972(3)	0.0336
C(16)	−0.0273(4)	0.2246(3)	0.6226(3)	0.0250
C(17)	−0.0810(4)	0.1278(3)	0.6383(3)	0.0296
O(111)	0.1967(4)	0.2773(2)	0.3709(3)	0.0376
O(112)	0.2038(4)	0.4267(2)	0.4040(3)	0.0410
O(171)	−0.0768(4)	0.0747(2)	0.5513(3)	0.0384
O(172)	−0.1272(4)	0.1047(2)	0.7225(3)	0.0428

[a] Equivalent isotropic *U*(iso) defined as one-third of the trace of the orthogonalized tensor.

Table 6. Selected Bond Distances (Å) and Angles (deg) for $[(dipicH)_2Fe^{II}_2(OH_2)_6]\cdot 2dipicH_2$ (**2**)

Fe(1)−O(120)	2.097(3)	Fe(1)−O(110)	2.277(3)
Fe(1)−O(130)	2.131(3)	Fe(1)−O(11)	2.307(2)
Fe(1)−O(11)	2.208(2)	Fe(1)−O(71)	2.488(3)
Fe(1)−N(1)	2.217(3)		
O(130)−Fe(1)−O(120)	89.4(1)	O(11)−Fe(1)−O(130)	84.0(1)
O(11)−Fe(1)−O(120)	151.2(1)	O(11)−Fe(1)−O(11)	68.9(1)
O(11)−Fe(1)−O(130)	93.5(1)	O(11)−Fe(1)−N(1)	141.2(1)
N(1)−Fe(1)−O(120)	135.5(1)	O(11)−Fe(1)−O(110)	84.4(1)
N(1)−Fe(1)−O(130)	98.4(1)	O(71)−Fe(1)−O(120)	69.8(1)
N(1)−Fe(1)−O(11)	72.4(1)	O(71)−Fe(1)−O(130)	87.6(1)
O(110)−Fe(1)−O(120)	82.9(1)	O(71)−Fe(1)−O(11)	138.86(9)
O(110)−Fe(1)−O(130)	166.8(1)	O(71)−Fe(1)−N(1)	66.8(1)
O(110)−Fe(1)−O(11)	88.2(1)	O(71)−Fe(1)−O(110)	99.6(1)
O(110)−Fe(1)−N(1)	94.6(1)	O(71)−Fe(1)−O(11)	151.65(9)
O(11)−Fe(1)−O(120)	83.0(1)		

(10) D'Ascenzo, G.; Marino A.; Sabbatini, M.; Bica, T. *Thermochim. Acta* **1978**, *25*, 325.

(11) (a) Hseu, J. F.; Chen, J. J.; Wei, H. H.; Cheng, M. C.; Wang, Y.; Yao, Y. D. *Inorg. Chim. Acta* **1991**, *184*, 1. (b) Cousson, A.; Nectoux, F. *Acta Crystallogr.* **1992**, *C48*, 1354.

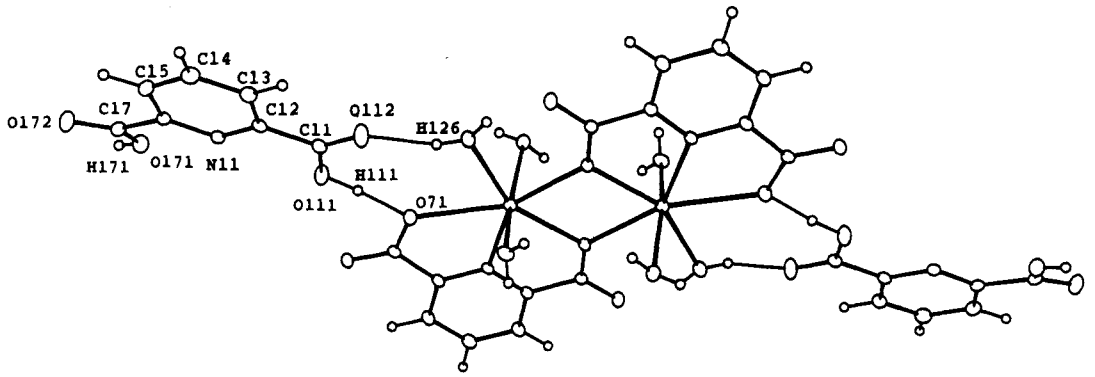

Figure 4. View of the asymmetric unit of **2** showing the hydrogen bonds between the complex and the two of dipicH_2 molecules.

and the oxygen atom O(120) lie in the same plane (the maximum deviation is less than 0.13 Å), and the directions Fe(1)−O(110) and Fe(1)−O(130) are nearly perpendicular to this plane with angles of 169.4 and 175.4°, respectively. This type of heptacoordination has been encountered in several other Fe^{II} complexes, in particular those with a macrocyclic ligand.[12] The metal to ligand bond distances in complex **2** are 0.1 Å larger than those observed in the isolated [(dipic)$Fe^{II}(OH_2)_3$].[8] Besides, as found in this latter complex, one of the iron−water distances is longer than the two others with Fe−O(110) = 2.277(3) Å, whereas Fe(1)−O(120) = 2.097(3) Å and Fe(1)−O(130) = 2.131(3) Å. As observed previously,[8] the shorter bond corresponds to the water molecules which are involved in intramolecular hydrogen bonding with H(127)−O(12) = 1.85(7) Å, O(120)−O(12) = 2.590(4) Å, H(126)−O(112) = 1.95(6) Å, O(120)−O(112) = 2.848(4) Å, and H(137)−O(72) = 1.98(7) Å, O(130)−O(72) = 2.735(4) Å. It should also be noticed that the Fe−O bond which is trans to the bridge is significantly longer [Fe(1)−O(71) = 2.488(3) Å] than those involving the bridging oxygen atoms [Fe(1)−O(11) = 2.208(2) Å and Fe(1)−O(11)′ = 2.307(2) Å].

The asymmetric unit also contains a dipicH_2 molecule, linked to the central complex molecule by two hydrogen bonds (Figure 4). One of them involves O(120), H(126), and O(112) as indicated above, while the other links O(111) and O(71) through the acidic H(111) with H(111)−O(71) = 1.50(6) Å and O(111)−O(71) = 2.487(4) Å. This dipicH_2 molecule is in a planar conformation, with only a small twist (3.95°) between the carboxylic group O(112)−C(11)−O(172) and the pyridine mean plane. This planar conformation is the most frequently encountered[13] in aromatic carboxylic acids involved in hydrogen bonding.

The formation of this complex is surprising in several regards. First it is a *nonprotonated complex,* while the pH at which it crystallizes is extremely low (1.35 at the end of the crystallization). Thus, this neutral complex is significantly less basic than the $[(dipic)_2Fe^{II}]^{2-}$ dianion, which would be transformed at this pH. Second, the oxygen atoms involved in the bridge are not those usually encountered in other multinuclear dipic/Fe complexes where each metal atom is linked to two different oxygen atoms of one carboxylate group. Third, it can be considered as a dimer of the [(dipic)Fe$(OH_2)_3$] complex described in paper 1 of this series. This is particularly surprising at first sight because a monomer/dimer equilibrium should evolve toward the dimer during the crystallization process. However, there is a major difference between the two systems: while [(dipic)$Fe^{II}(OH_2)_3$] crystallizes alone, $[(dipic)_2Fe^{II}_2(OH_2)_6]$ crystallizes with two dipicH_2 molecules which are connected to the complex by hydrogen bonds. This could be sufficient to stabilize the dimeric complex in the solid state.

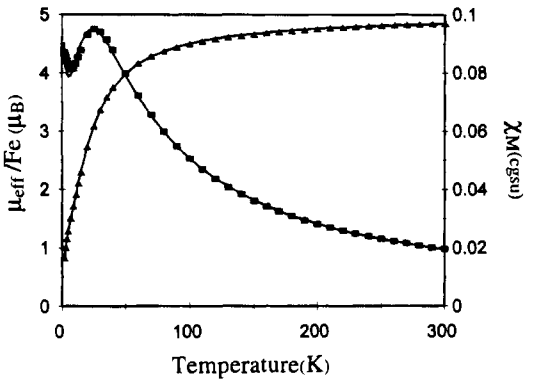

Figure 5. Variable-temperature magnetic susceptibility data for $[(dipic)Fe^{II}(OH_2)_3]_2$. The solid lines result from a least-squares fit of the data to the theoretical magnetic susceptibility calculated as mentioned in the text.

Magnetic Properties. The temperature dependence of the magnetic susceptibility and effective magnetic moment per iron of $[(dipic)Fe^{II}(OH_2)_3]_2$ are shown in Figure 5. μ_{eff}/Fe decreases from 4.85 μ_B at 300 K to 0.83 μ_B at 2 K, indicating a weak antiferromagnetic coupling of the $S = 2$ spin systems of the two ferrous ions of each dinuclear unit and possibly single-ion zero-field splitting (ZFS). As previously discussed (X-ray crystal structure determination section), both ligands of the dimeric unit of $[(dipic)Fe^{II}(OH_2)_3]_2$ bridge Fe(1) to Fe(1)′ through the oxygen carboxylate atoms O(11) and O(11)′ affording an intradimer Fe−Fe separation of 3.645(4) Å. The coordination polyhedron around the symmetry-related Fe and Fe′ cations can be described as a distorted pentagonal bipyramid with individual z axes along the O(110)−O(130) directions. Since the Fe−Fe distance is too large to allow direct overlap between d orbitals, the only effective exchange pathway involves probably superexchange through the $O_{carboxylato}$ bridges.

We have thus initially analyzed the variation of the magnetic susceptibility of $[(dipic)Fe^{II}(OH_2)_3]_2$ by employing the expression derived from the isotropic spin-exchange Hamiltonian $H = -2JS_1S_2$ ($S_1 = S_2 = 2$) and the Van Vleck equation, modified to allow admixture of paramagnetic impurity.[14] Although the least-squares refinements obtained with this model afforded a reasonable fit for $J \sim -4$ cm^{-1} in the high-temperature range, it was poor below 40 K. The least-squares fit of the experimental data to the temperature-dependent molar magnetic susceptibility (expressed according to the above equation modified to take into account interdimer interactions in the

(12) Drew, M. G. B.; Bin Othman, H.; McFall, S. G.; Mc Lloyd, P. D. A.; Nelson, S. M. *J. Chem. Soc., Dalton Trans.* **1977**, 1173
(13) O'Connor, C. J. *Prog. Inorg. Chem.* **1982**, *29*, 203.
(14) Ginsberg, A. P.; Lines, M. E. *Inorg. Chem.* **1972**, *11*, 2289.

molecular field approximation[15]) did not afford better results. The inability of the two methods to account for the experimental results indicates that the antiferromagnetic behavior of $[(dipic)Fe^{II}(OH_2)_3]_2$ cannot be interpreted by considering only isotropic exchange interactions. The experimental results suggesting that the magnetic exchange interactions are weak, the crystalline field anisotropy, and the magnetic exchange interactions are expected to be of the same order of magnitude. Consequently, we attempted to fit the experimental data to the theoretical magnetic susceptibility calculated by exact diagonalization of the effective spin Hamiltonian taking into account single-ion ZFS.[15] The least-squares refinement of the experimental data to the theoretical magnetic susceptibility calculated from this model afforded a very good fit (Figure5) for the parameters, $J = -3.4\ cm^{-1}$, $D = -3.1\ cm^{-1}$, $g_\perp = 1.999$, $g_{||} = 2.074$, and Par = 1.7%, where Par is the mole percent of a paramagnetic impurity assumed to be a Fe(III) monomer. The absolute value obtained for D clearly indicates that the magnetic behavior of $[(dipic)Fe^{II}(OH_2)_3]_2$ is relevant to the case where the ZFS of the single ion is of the order of magnitude of the exchange integral and cannot be treated as a perturbation. The fact that a reasonable fit could only be obtained for a negative D value indicates that the anisotropy of the ligand field is similar to that originating from an axial elongation in the case of a coordination octahedron. In these regards, it is interesting to notice that an increased number of equatorial versus apical ligands (which is the case for a pentagonal bipyramid compared to a regular octahedron) should have formally the same effect on the ligand field at the iron center as the axial elongation of an octahedron.

The bridging mode of the ferrous ions through the oxygen carboxylate atoms of both ligands in $[(dipic)Fe^{II}(OH_2)_3]_2$ is very similar to that observed in $[Fe^{II}(L^2)(Cl)(MeOH)_2]_2$ (wherein L^2H is an analog of pyrroloquinoline quinone).[16] The Fe−Fe distances (3.724(1) and 3.645(4) Å, respectively) and the Fe−$O_{carboxylato}$−Fe angles (111.1(1) and 109.2(1)°, respectively) are close in these two compounds, which is reflected by the sign and values of the J isotropic exchange integrals (−3.4 and −2.1 cm^{-1}, respectively). However, the symmetry of the coordination spheres is very different (pentagonal bipyramid in the former and axially compressed octahedron in the latter) as shown by the significant difference in magnitude and sign of the D crystalline field anisotropy parameters (−3.1 and +11.1 cm^{-1}, respectively).

Correlation with Solution Chemistry. Since there seems to be a relation between heptacoordination and protonation, we investigated the solution behavior upon protonation of $[(dipic)_2Fe^{II}]^{2-}$.

Figure 6 shows the variation of the optical density of an aqueous 8.9×10^{-3} M solution of $[(dipic)_2Fe^{II}]Na_2{\cdot}2H_2O$ as a function of the number of H^+ equivalent added to this solution at room temperature. It shows an angular point at $n_{equiv}(H^+) = 0.5$ (the pH is around 3), which indicates that the acidification proceeds in at least two steps; the angular point could correspond to the consumption of one proton for two complexes according to the equation

$$2[(dipic)_2Fe^{II}]^{2-} + H^+ \rightarrow [(dipic)_3(dipicH)Fe^{II}{}_2]^{3-}$$

Such a formula requires a dimerization of the complex induced by protonation. As shown for $[(dipicH)_2Fe^{II}(OH_2)]$, the protonation of a carboxylate group could allow the coordination of a seventh ligand to Fe^{II}; this ligand must be the carboxylato oxygen atom of an another complex, giving for $[(dipic)_3(dipicH)Fe^{II}{}_2]^{3-}$ the structure shown in Figure 7.

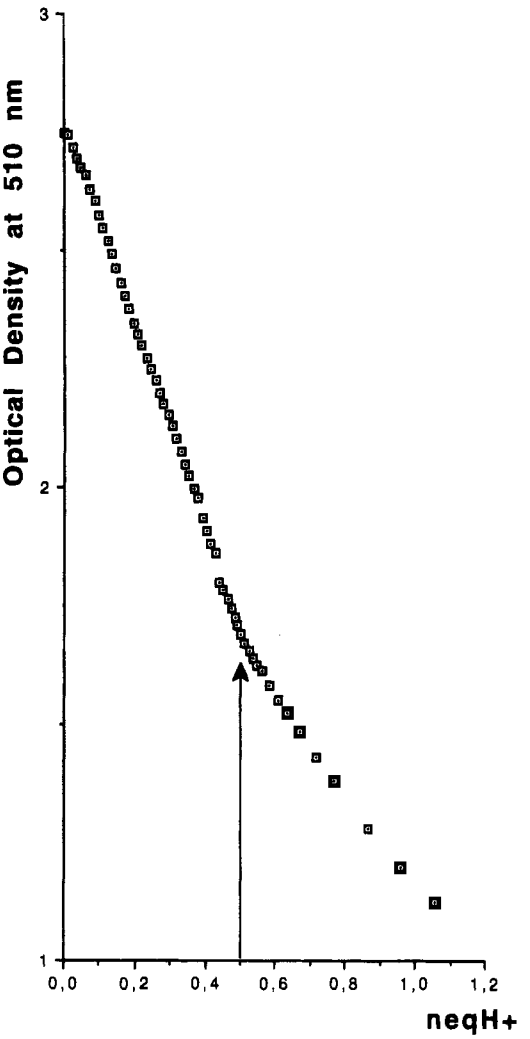

Figure 6. Variation of the optical density of an aqueous 8.9×10^{-3} M solution of $[(dipic)_2Fe^{II}]Na_2{\cdot}2H_2O$ as a function of the number of added equivalent H^+.

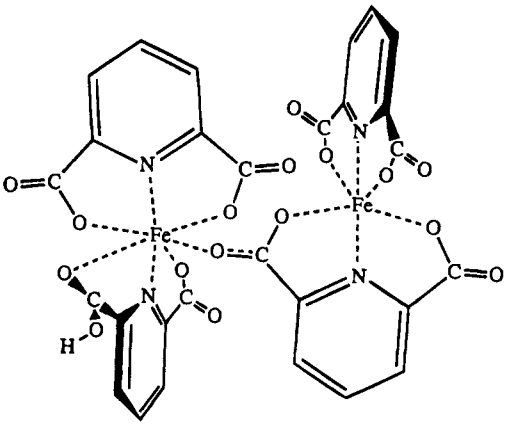

Figure 7. Hypothetical structure of the dimer $[(dipic)_3(dipicH)Fe^{II}{}_2]^{3-}$.

A final comment can be made about the use of iron dipic complexes in some catalytic processes. Some protonated complexes such as $[(dipicH)_2Fe^{II}]$ have been frequently invoked as reactive intermediates or precursors.[17] Our work casts doubt on the uniqueness or even the existence of such species in solution.

(15) Garge, P.; Chikate, R.; Padhye, S.; Savariault, J. M.; De Loth, P.; Tuchagues, J. P. *Inorg. Chem.* **1990**, *29*, 3315.
(16) Tommasi, L.; Shechter-Barloy, L.; Varech, D.; Battioni, J.-P.; Donnadieu, B.; Verelst, M.; Bousseksou, A.; Mansuy, D.; Tuchagues, J.-P. *Inorg. Chem.* **1995**, *34*, 1514.

Conclusion

Two new heptacoordinated Fe^{II} complexes have been obtained by acidic degradation of $[(dipic)_2Fe^{II}]^{2-}$ or species deriving formally from this compound: (i) the monuclear complex $[(dipicH)_2Fe^{II}(OH_2)]$, in which protonation of two dipic ligands allows the coordination of a solvent molecule leading to a capped octahedral geometry; (ii) the dinuclear $[(dipic)_2Fe^{II}_2(OH_2)_6]\cdot 2dipicH_2$, which results formally from the loss of one dipic ligand after protonation and subsequent dimerization. In this compound, the ligands around Fe^{II} are in a pentagonal bipyramid geometry.

Acknowledgment. The authors thank A. Mari for carrying out the magnetic susceptibility measurements.

Supporting Information Available: Complete tables of X-ray crystallographic parameters, atomic coordinates, thermal parameters, bond lengths, and bond angles for complexes **1** and **2** and detailed data resulting from the magnetic susceptibility measurements for complex **2** in the 300−2 K temperature range (12 pages). Ordering information is given on any current masthead page.

IC950103W

(17) (a) Sheu, C. *J. Am. Chem. Soc.* **1990**, *112*, 8212. (b) Sheu, C.; Sobkowiak, A.; Jeon, S.; Sawyer, D. T. *J. Am. Chem. Soc.* **1990**, *112*, 879.